Charged current neutrino-nucleus reaction cross sections at intermediate energies

T. S. Kosmas*
Division of Theoretical Physics, University of Ioannina, GR-451 10 Ioannina, Greece

E. Oset
Departamento de Fisica Teorica and Instituto de Fisica Corpuscular, Centro Mixto Universidad de Valencia, Consejo Superior de Investigaciones Cientificas, 46100, Burjassot (Valencia), Spain
(Received 16 October 1995)

Inclusive and semi-inclusive neutrino-nucleus reaction cross sections at intermediate energies (20 MeV $\leqslant E_\nu \leqslant$ 500 MeV) are calculated throughout the Periodic Table for the most interesting nuclei from an experimental point of view. The method used had previously proved to be very accurate in calculating the inclusive reaction cross section for light nuclei (^{12}C and ^{16}O) and in the study of other similar processes and has been further improved to deal with low energy neutrinos. The electron neutrino (ν_e) and muon neutrino (ν_μ) cross sections weighted by their energy distributions are also calculated and discussed in conjunction with the existing experimental results at LAMPF and the KARMEN Collaboration.

PACS number(s): 25.30.Pt, 13.15.+g

I. INTRODUCTION

The study of total cross sections in the neutrino-nucleus reactions

$$\nu_l + (A,Z) \rightarrow l^- + X, \bar{\nu}_l + (A,Z) \rightarrow l^+ + X, l = e, \mu \qquad (1)$$

is of great importance in neutrino detection [1–5], in particular for nuclear targets used in the existing neutrino detectors [1,6] and promising nuclear isotopes proposed [2] to be used as neutrino detection targets [6,7]. For the existing detectors it is interesting to know reliable estimates of the neutrino-nucleus cross section for E_ν at least up to a few hundred MeV, e.g., for the radiochemical experiments we need semi-inclusive cross sections while for the Cerenkov or liquid scintillation experiments we need inclusive reaction cross sections. On the other hand, for reactions of neutrinos with some nuclei proposed as promising nuclear targets in neutrino detectors [2], such as ^{81}Br, ^{98}Mo, ^{115}In, ^{127}I, ^{205}Tl, the knowledge of a reliable cross-section calculation is a fundamental prerequisite [7–13].

So far, neutrino-nucleus cross sections have been calculated for some nuclear targets by using the following methods.

(i) Term-by-term sum [14]: This method needs the explicit construction of the final states in the context of a nuclear model and it is reliably applicable for low neutrino energies for light and medium nuclei when the transitions to definite nuclear states (ground-state or some low-lying excitations) could be dominant.

(ii) Closure approximation [15]: With this method one avoids the tedious construction of the excited nuclear states if a suitable mean excitation energy $\bar{E}$ could be chosen. The results of this method depend on the assumed value of $\bar{E}$ and it is more reliable for neutrino energies 50 MeV$\leqslant E_\nu \leqslant$100 MeV.

(iii) Fermi gas models [16]: The use of the non-relativistic or relativistic Fermi gas model needs a choice of the average binding energy which defines the effective energy transfer to the nuclear target. The results are very sensitive to the average binding energy used (in particular at low neutrino energies) and more reliable estimates for neutrino cross sections can be obtained for $E_\nu \geqslant 50$ MeV where the details of the specific nuclear states can be ignored.

(iv) Recently [4,17], a new method has been developed in which the differential neutrino nucleus cross section can be expressed as a function of the local Fermi momentum $p_F(r)$, i.e., by using a local density approximation. In this way both bound as well as excited states of the proton and neutron can be taken into account by using the particle-hole excitations included in a relativistic Lindhard function [4]. In addition, one can also consider the very important effects of Coulomb distortion and renormalization of the operators involved in the elementary neutrino nucleon process inside the nucleus [18–20].

In the present work we have improved method (iv) [4] and calculated total cross sections for the inclusive and semi-inclusive neutrino reactions of Eq. (1) throughout the Periodic Table. In this version method (iv) takes into consideration the gap for a minimum excitation energy of the final nucleus. Obviously, in infinite nuclear matter this gap is zero but in the case of a finite nuclear system this value varies from $\approx$6 MeV, for light nuclei, to $\approx$2–3 MeV, for heavy nuclei. This is accounted for by means of the modified Lindhard function, discussed in Ref. [21], which we have used in the present calculations. A second improvement of the method has been done so that it can give us the cross sections for particle-bound nuclear states with which we have calculated the flux-averaged cross section for radiochemical experiments.

We have studied total neutrino-nucleus cross sections for the most important nuclear isotopes in neutrino detection in

*Present address: Institute of Theoretical Physics, University of Tübingen, D-72076, Germany.

the energy region 20 MeV$\leqslant E_\nu \leqslant$500 MeV. These neutrino energies, which cover the high energy supernova neutrinos, the solar flare neutrinos, etc., can excite good enough nuclear states such that, the integration over the continuum involved in the method used here is a very good approximation for $E_\nu \geqslant 50$ MeV, in the region of light nuclei, and for $E_\nu \geqslant 20$ MeV, in the region of medium and heavy nuclei.

The calculated cross sections are useful in the study of atmospheric neutrinos which carry neutrino energies between a few MeV to some GeV and can be observed, e.g., in a large water Cerenkov detector. Also the interesting quantity of the ratio of the muon-neutrino flux to that of the electron-neutrino flux for atmospheric neutrinos can be calculated by using the results of total neutrino cross sections.

From the neutrino cross sections obtained we have calculated the experimentally important ''flux-averaged cross sections'' and compared them with the corresponding values found for various electron- and muon-neutrino reactions in the KARMEN [8,9] and LAMPF [10–13] Collaborations.

II. BRIEF DESCRIPTION OF THE FORMALISM

For the neutrino-induced reactions of Eq. (1) the effective transition operator $H_{\rm eff}$ can be written in a covariant form as

$$H_{\rm eff}=\frac{G\cos\theta_c}{\sqrt{2}} j^\mu J_\mu , \tag{2}$$

where G is the weak coupling constant ($G=1.1664\times10^{-5}$ GeV^{-2}) and θ_c the Cabibbo angle ($\cos\theta_c=0.974$). The leptonic current j^μ is the familiar one

$$j^\mu=\bar{u}_l(p_l)\gamma^\mu(1-\gamma_5)u_\nu(p_\nu), \tag{3}$$

where u_ν, u_l are Dirac spinors for the neutrino and lepton having four-momentum p_ν, p_l, respectively, with the normalization $\bar{u}u=1$. The hadronic current J_μ in Eq. (2) is given by [4]

$$J_\mu=\bar{u}_p(p_p)\left[F_1(q^2)\gamma_\mu+F_2(q^2)i\sigma_{\mu\lambda}\frac{q^\lambda}{2M}+F_A(q^2)\gamma_\mu\gamma_5 + F_P(q^2)q_\mu\gamma_5\right]u_n(p_n) \tag{4}$$

(M is the nucleon mass). The functions of the four-momentum transfer q^2 (with $q=p_p-p_n$): F_1, F_2, F_A, and F_P are the well-known Dirac, Pauli, axial vector, and pseudoscalar form factors, respectively. In the convention used in the present work q^2 is written as

$$q^2=q^\mu q_\mu=q_0^2-\mathbf{q}^2=(E_l-E_\nu)^2-(\mathbf{p}_l-\mathbf{p}_\nu)^2. \tag{5}$$

$\mathbf{p}_i$ denotes the three-momentum of the particles involved in the process.

For the antineutrino-induced reaction the leptonic and hadronic currents are the complex conjugates of Eqs. (3) and (4), respectively.

A. The local density approximation

The calculation of the total neutrino-nucleus reaction cross section σ, according to method (iv) mentioned in the Introduction and modified as indicated below, is given by [4]

$$\sigma=-\frac{2G^2\cos^2\theta_c}{\pi}\int_0^R r^2dr\int_{p_l^{\min}}^{p_l^{\max}}p_l^2dp_l \times\int_{-1}^{1}d(\cos\theta)\frac{1}{E_\nu E_l}\overline{\sum}\sum|T|^2\bar{\rm Im}U[E_\nu-E_l -Q+Q_{\rm th}-V_C(r),\mathbf{q}]\Theta[E_l+V_C(r)-m_l], \tag{6}$$

where the quantity $\overline{\sum}\sum|T|^2$ represents the sum and average over final and initial spins of the leptons and nucleons (for the analytic form of $|T|^2$ see Appendix of Ref. [4]). The function $\Theta[E_l+V_C(r)-m_l]$ is the *theta* function, V_C is the Coulomb energy of the lepton, and Q is the Q value of the process. The function $\bar{\rm Im}U(q^0,\mathbf{q})$ represents the imaginary part of the modified Lindhard function [21] which contains the particle-hole excitation of proton-neutron type. The minimum ($p_l^{\min}=0$) and maximum $\{p_l^{\max}=[(E_l^{\max})^2-m_\mu^2]^{1/2}\}$ lepton momentum are determined by the kinematics, i.e.,

$$E_l^{\max}=E_\nu-V_C(r)-Q. \tag{7}$$

The quantity $Q_{\rm th}$ in Eq. (6) is the difference of the proton and neutron local Fermi energies

$$Q_{\rm th}=E_{p_F}-E_{n_F}. \tag{8}$$

In the local density approximation, the magnitude of the momenta p_{F_n} and p_{F_p} are given in terms of the neutron and proton nuclear densities $\rho_n(r)$ and $\rho_p(r)$, respectively, as

$$p_{F_n}=[3\pi^2\rho_n(r)]^{1/3},\quad p_{F_p}=[3\pi^2\rho_p(r)]^{1/3}. \tag{9}$$

In a good approximation ρ_n and ρ_p are obtained from the total charge density of the nucleus $\rho(r)$ via the relations $\rho_n(r)=\rho(r)N/A$ and $\rho_p(r)=\rho(r)Z/A$. In Eq. (6) we let R take the value $R=C_1+5$ fm where C_1 represents the radius parameter of a two-parameter Fermi density distribution (see Table I below).

In the case of the neutrino reaction of Eq. (1) the total energies of the neutron (E_n) and proton (E_p) are written as

$$E_n=\sqrt{\mathbf{p}_n^2+M_n^2},$$
$$E_p=\sqrt{(\mathbf{p}_n+\mathbf{q})^2+M_p^2}\approx\sqrt{\mathbf{p}_n^2+\mathbf{q}^2+M_p^2}, \tag{10}$$

where the approximation in E_p holds if $\mathbf{q}\cdot\mathbf{p}_n\approx0$.

For the antineutrino-nucleus process, since in this case the role of the proton and neutron is interchanged (we neglect the proton-neutron mass difference), one can calculate the cross section by using the same expression for $|T|^2$ as for neutrino scattering and changing the sign of terms involving the products F_1F_A and F_2F_A in the expression of the Appendix of Ref. [4]. In addition $Q_{\rm th}$ will have an opposite sign to the one of Eq. (8).

The renormalization of the currents mentioned in the Introduction is done by allowing the propagation of the ph in

TABLE I. Characteristics of some neutrino- and antineutrino-nucleus reactions employed in neutrino detection. C_1 (radius parameter) and C_2 (thickness parameter) describe a two-parameter Fermi density distribution of the target nucleus and Q (in MeV) represents the Q value of the corresponding reaction, equal to $M(A,Z+1)-M(A,Z)$, for neutrino scattering and $M(A,Z-1)-M(A,Z)$, for antineutrino scattering, where (A,Z) refers to the original nucleus.

Nucleus	Density Parameters		Neutrino processes		Antineutrino processes	
${}^{A}_{N}X$	C_1	C_2	Reaction	Q	Reaction	Q
${}^{37}_{17}$Cl	3.535	0.524	${}^{37}_{17}\mathrm{Cl}(\nu_l,l^-){}^{37}_{18}\mathrm{Ar}$	0.303	${}^{37}_{17}\mathrm{Cl}(\bar{\nu}_l,l^+){}^{37}_{16}\mathrm{S}$	5.365
${}^{40}_{18}$Ar	3.530	0.542	${}^{40}_{18}\mathrm{Ar}(\nu_l,l^-){}^{40}_{19}\mathrm{K}$	0.994	${}^{40}_{18}\mathrm{Ar}(\bar{\nu}_l,l^+){}^{40}_{17}\mathrm{Cl}$	8.006
${}^{71}_{31}$Ga	4.445	0.580	${}^{71}_{31}\mathrm{Ga}(\nu_l,l^-){}^{71}_{32}\mathrm{Ge}$	−0.276	${}^{71}_{31}\mathrm{Ga}(\bar{\nu}_l,l^+){}^{71}_{30}\mathrm{Zn}$	3.328
${}^{81}_{35}$Br	4.640	0.572	${}^{81}_{35}\mathrm{Br}(\nu_l,l^-){}^{81}_{36}\mathrm{Kr}$	−0.189	${}^{81}_{35}\mathrm{Br}(\bar{\nu}_l,l^+){}^{81}_{34}\mathrm{Se}$	2.096
${}^{98}_{42}$Mo	5.107	0.569	${}^{98}_{42}\mathrm{Mo}(\nu_l,l^-){}^{98}_{43}\mathrm{Tc}$	1.169	${}^{98}_{42}\mathrm{Mo}(\bar{\nu}_l,l^+){}^{98}_{41}\mathrm{Nb}$	4.074
${}^{115}_{49}$In	5.357	0.563	${}^{115}_{49}\mathrm{In}(\nu_l,l^-){}^{115}_{50}\mathrm{Sn}$	−1.005	${}^{115}_{49}\mathrm{In}(\bar{\nu}_l,l^+){}^{115}_{48}\mathrm{Cb}$	1.959
${}^{127}_{53}$I	5.405	0.552	${}^{127}_{53}\mathrm{I}(\nu_l,l^-){}^{127}_{54}\mathrm{Xe}$	0.152	${}^{127}_{53}\mathrm{I}(\bar{\nu}_l,l^+){}^{127}_{52}\mathrm{Te}$	1.206
${}^{205}_{81}$Tl	6.495	0.540	${}^{205}_{81}\mathrm{Tl}(\nu_l,l^-){}^{205}_{82}\mathrm{Pb}$	−0.451	${}^{205}_{81}\mathrm{Tl}(\bar{\nu}_l,l^+){}^{205}_{80}\mathrm{Hg}$	2.049

the nuclear medium. The ph response is substituted by an RPA response accounting for ph and delta-hole components which interact by means of the spin-isospin effective nuclear interaction. This renormalization procedure took good account of the renormalization of the currents in muon capture [18] and in beta decay [19].

With respect to Ref. [4] the present formalism has incorporated the use of the modified Lindhard functions $\bar{U}(q^0,\mathbf{q})$ of Ref. [21]. The use of this function becomes necessary when studying the neutrino cross sections at low energies. The reason for it is that, the ordinary Lindhard function [22] has a pathological behavior at $q^0=0$ and $\mathbf{q}\to 0$. Let us see this. The ordinary Lindhard function [22] for p,n excitation is given by

$$\bar{U}(q^0,\mathbf{q})=2\int\frac{d^3p}{(2\pi)^3}\left\{\frac{n(\mathbf{p})[1-n(\mathbf{p}+\mathbf{q})]}{q^0+\varepsilon(\mathbf{p})-\varepsilon(\mathbf{p}+\mathbf{q})+i\epsilon}+\frac{n(\mathbf{p})[1-n(\mathbf{p}-\mathbf{q})]}{-q^0+\varepsilon(\mathbf{p})-\varepsilon(\mathbf{p}-\mathbf{q})+i\epsilon}\right\},\tag{11}$$

where $n(\mathbf{p})$ is the occupation number of the Fermi sea and $\varepsilon(\mathbf{p})$ the nucleon kinetic energy.

When $q^0=0$ and in the limit of $\mathbf{q}\to 0$, Eq. (11) leads to an expression of the type 0/0 which has a finite limit, and actually $|\mathrm{Re}\bar{U}(0,q\to 0)|$ has a maximum there. However, the response function for a finite nucleus with closed shells is zero, since one has matrix elements of the type $\langle n|e^{i\mathbf{q}\cdot\mathbf{r}}|0\rangle$, with $|0\rangle$ the ground state and $|n\rangle$ standing for excited states. This matrix element vanishes for $\mathbf{q}\to 0$. Hence the disagreement between nuclear matter and finite nuclei in this limit is extreme. Actually, the numerator of Eq. (11) vanishes when $\mathbf{q}\to 0$. The difference between a Fermi sea and the finite nucleus is that the denominator of Eq. (11) vanishes when $q^0=0$ and $\mathbf{q}\to 0$, while in finite nuclei it does not. This is because in nuclear matter one has a continuum of states while in finite nuclei there is a minimum energy needed to excite the first excited state. This gap of energy is what makes the denominator of the response function different from zero for finite nuclei.

In view of this, the Lindhard function was modified [21] to account for the gap of the excited states and we have used it here. The use of this modified Lindhard function has been essential to cure some numerical pathologies which appeared in the evaluation of the neutrino cross section at low energies for some nuclei.

The pathologies disappear throughout the Periodic Table as soon as a gap of around 1 MeV is used and the results are then not much sensitive to the precise value of the gap used. Since the purpose of the gap is to avoid the numerical instabilities we have used a constant value for the gap, rather than using a precise value for each nucleus. For this value we have chosen 3 MeV, which already provides very stable results. As an example, taking instead a gap of 6 MeV changes the cross sections below the level of 2% in all the range of energies and nuclei studied.

B. Michel distribution

The electron neutrino beams used in experiments (e.g., at LAMPF, KARMEN, etc.) are produced from the decay of muons resulting from the decay of slow pions and therefore they have relatively low energies. Such neutrinos do not constitute a monochromatic beam. Their energy distribution is approximately described by the Michel distribution

$$\frac{dN_\nu}{dE_\nu}\equiv W(E_\nu)\approx E_\nu^2(E_\nu^{\max}-E_\nu),\tag{12}$$

where

$$E_\nu^{\max} \approx \frac{m_\mu^2 - m_e^2}{2m_\mu}. \quad (13)$$

For comparison of the theoretical semi-inclusive cross section with experimental data we can calculate the flux-averaged cross section given by

$$\bar{\sigma} = \frac{\int_0^{E_\nu^{\max}} \sigma(E_\nu) W(E_\nu) dE_\nu}{\int_0^{E_\nu^{\max}} W(E_\nu) dE_\nu}. \quad (14)$$

The numerator of Eq. (14) represents the folding of the neutrino cross section with the energy distribution of Eq. (12). The denominator stands for normalization requirements. The maximum energy in the upper limit of this integral is $E_\nu^{\max} \approx 52.8$ MeV.

In order to obtain $\bar{\sigma}$ in the case of muon neutrinos one can make the same average as in Eq. (14) with the distribution of neutrinos given in Refs. [12,13], and put $E_\nu^{\max} \approx 280.0$ MeV.

III. DESCRIPTION OF NEUTRINO DETECTION REACTIONS

In the present work we deal with the neutrino-nucleus cross sections of eight nuclei which have been considered important in neutrino detection experiments. The basic reactions and the quantities needed for the present calculations are shown in Table I [23,24]. The nuclear distribution parameters (columns 2 and 3) refer to a two-parameter Fermi density which we have used in Eq. (6). These parameters either have been obtained directly from experimental data [23] or by interpolation using the experimental data [23] and Ref. [20].

The important role which each of the isotopes plays studied here in neutrino detection is discussed in detail in other works [5–7]. However, we find it helpful to the reader to mention some of their characteristics. The majority of these nuclides ^{37}Cl, ^{71}Ga, ^{81}Br, ^{98}Mo, ^{127}I, and ^{205}Tl, is appropriate for experiments of radiochemical type, while ^{40}Ar and ^{115}In can be employed in direct counting experiments. Moreover, the ^{37}Cl detector, operating since many years ago at Homestake [1,7], is sensitive only to neutrino energies above $E_{\rm thres} = 0.814$ MeV. The two ^{71}Ga solar neutrino detectors, at [6] Gran Sasso and Baksan, have a threshold of only 0.233 MeV and have been used for measuring the flux of p-p neutrinos. The ^{81}Br, proposed as a solar neutrino detector [7], has a threshold energy $E_{\rm thres} = 0.471$ MeV. The ^{127}I can be used as a promising solar neutrino candidate to cover the region between ^{71}Ga and the water detector Cerenkov chamber. Measurements of ^{127}I can be used to calibrate the cross sections of the ^{8}B and ^{7}Be neutrinos, since ^{127}I is sensitive to both of them. At present an experiment with ^{127}I is under way at LAMPF (see Sec. IV).

The two promising detectors ^{205}Tl and ^{98}Mo could be used in geochemical experiments. The one with ^{98}Mo has already been developed in LAMPF, since the ^{98}Mo detector could be used for measuring the flux of ^{8}B neutrinos averaged over the past several milion years. The threshold for the neutrino reaction $^{98}\mathrm{Mo}(\nu_e, e^-)^{98}\mathrm{Tc}$ is $E_{\rm thres} = 1.68$ MeV but, because the ground state and the first excited state of ^{98}Tc are forbidden, effectively $E_{\rm thres} > 1.74$ MeV. The use of ^{205}Tl as a solar neutrino detector would have the smallest threshold energy, $E_{\rm thres} = 0.062$ MeV, which reflects its sensitivity in p-p neutrinos. The proposal for a geochemical experiment with ^{205}Tl [5] suggests the measure of the concentration of the ^{205}Pb isotope produced by solar neutrinos in natural ores.

From the promising direct counting detectors, the liquid ^{40}Ar detector at Gran Sasso (ICARUS experiment) is optimized to observe solar neutrinos and it has a threshold energy $E_{\rm thres} = 5.885$ MeV. The ^{115}In isotope has been proposed [2] as a liquid scintillator solar neutrino detector, because it has a very low threshold $E_{\rm thres} = 0.119$ MeV. The produced ^{115}Sn is in the second excited ($\frac{7}{2}^+$) state.

Before closing this section we should mention that from the corresponding (p,n) reactions of the above nuclides the Gamow-Teller strengths are determined, from which the cross sections for solar neutrino absorption have been calculated [7].

IV. RESULTS AND DISCUSSION

The main goal of the present work was the calculation of inclusive and semi-inclusive neutrino and antineutrino-nucleus cross sections throughout the Periodic Table with the accurate method of Ref. [4], modified as discussed in Sec. II. To our knowledge no systematic study of the inclusive and semi-inclusive cross section for intermediate neutrino energies has been carried up to now.

The results of the total cross sections as a function of neutrino energies E_ν for eight nuclear targets are presented in Fig. 1. These results enable us to study the dependence of the neutrino-nucleus cross section on the nuclear charge Z and mass A. The common characteristics of the cross sections shown in Fig. 1 is that they rise appreciably at low energies but the growth becomes moderate at higher energies. In the same nucleus there are differences between the neutrino and antineutrino reactions but for each target the electron neutrino cross sections in the region $300 \leqslant E_\nu \leqslant 500$ MeV are about equal to the corresponding muon-neutrino cross sections and the electron-antineutrino cross sections are about equal to those of the muon antineutrino.

There are few experimental data to compare with in this energy regime. One of the reactions for which there are measurements is the ν_e cross section on ^{12}C both from the KARMEN [8,9] and Los Alamos Collaborations [10,11]. The cross sections are the averaged ones with the Michel distribution, and although there are still some discrepancies in the amount of strength that goes into the excitation of the ^{12}N (g.s) and the excited states, the total ν_e cross section is about the same in both experiments (see Table II). In the present work, by using our modified method, we have repeated the calculation done for $\bar{\sigma}$ of ^{12}C in Ref. [4]. Our results, with a cross section of $\bar{\sigma} = 0.14 \times 10^{-40}$ cm^2 agree well with experiments. In Ref. [4] we make a thorough discussion of the results of other methods and we omit this here.

Recently, there have been some measurements in ^{127}I at Los Alamos. They have the peculiarity of being experiments of radiochemical type. This means that the ^{127}Xe in the final state is chemically separated. Hence, this kind of experiment includes all final states in which the ground state of ^{127}Xe or any excited state of this element (which will go to the ground state by radiative decay) are produced.

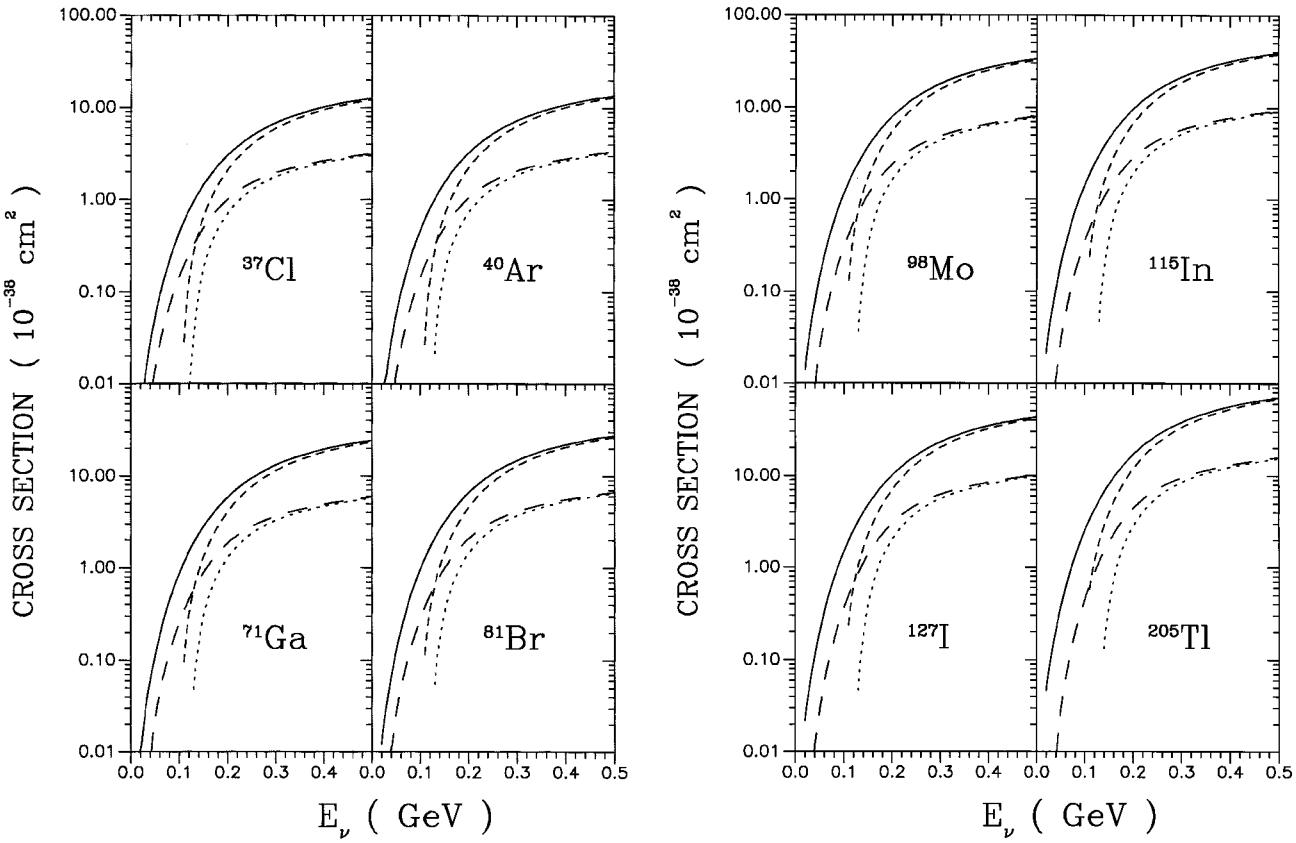

FIG. 1. Total cross sections of neutrino-nucleus induced reactions for certain promising neutrino detection nuclear targets. The curves plotted refer to the reactions: $(A,Z)(\nu_e,e^-)(A,Z+1)$ (solid line), $(A,Z)(\nu_\mu,\mu^-)(A,Z+1)$ (long-dashed line), $(A,Z)(\bar{\nu}_e,e^+)(A,Z-1)$ (short-dashed line), and $(A,Z)(\bar{\nu}_\mu,\mu^+)(A,Z-1)$ (dotted line).

TABLE II. Flux-averaged cross section $\bar{\sigma}$ for ν_e obtained by folding the cross section σ in a Michel neutrino energy distribution [see Eq. (14)]. Column indicated as ''Radiochemical'' contains only the contribution of particle bound states of the final nucleus.

		Average cross section $\bar{\sigma}$ (10^{-40} cm^2)			
(A,Z)	Reaction	Total	Radio-chemical	KARMEN expt.	LAMPF expt.
$^{12}_{6}$C	$^{12}_{6}$C$(\nu_e,e^-)^{12}_{7}$N	0.14	-	0.15±0.03 Ref. [9]	0.14±.03 Ref. [10]
$^{37}_{17}$Cl	$^{37}_{17}$Cl$(\nu_e,e^-)^{37}_{18}$Ar	1.8	1.4		
$^{40}_{18}$Ar	$^{40}_{18}$Ar$(\nu_e,e^-)^{40}_{19}$K	1.9	1.3		
$^{71}_{31}$Ga	$^{71}_{31}$Ga$(\nu_e,e^-)^{71}_{32}$Ge	4.0	2.7		
$^{81}_{35}$Br	$^{81}_{35}$Br$(\nu_e,e^-)^{81}_{36}$Kr	4.5	3.2		
$^{98}_{42}$Mo	$^{98}_{42}$Mo$(\nu_e,e^-)^{98}_{43}$Tc	5.3	2.7		
$^{115}_{49}$In	$^{115}_{49}$In $(\nu_e,e^-)^{115}_{50}$Sn	7.2	4.7		
$^{127}_{53}$I	$^{127}_{53}$I$(\nu_e,e^-)^{127}_{54}$Xe	7.3	4.3		6.2±2.5 Ref. [11][a]
$^{205}_{81}$Tl	$^{205}_{81}$Tl $(\nu_e,e^-)^{205}_{82}$Pb	14.0	6.3		

[a] [a]This experiment is of a radiochemical type.

TABLE III. Energies for proton emission $E^p_{\rm thres} = M(A'-1,Z'-1)+M_p-M(A',Z')$ and neutron emission $E^n_{\rm thres} = M(A'-1,Z')+M_n-M(A',Z')$, for certain neutrino detection targets. (A',Z') represents the daughter nucleus in the reaction.

Nucleus (A,Z)	Proton emission $E^p_{\rm thres}$ (MeV)	Neutron emission $E^n_{\rm thres}$ (MeV)
(12, 7)	0.6	15.97
(37,18)	8.72	8.80
(40,19)	7.58	7.81
(71,32)	8.29	7.43
(81,36)	9.05	7.83
(98,43)	6.18	7.29
(115,50)	8.75	7.56
(127,54)	7.70	7.24
(205,82)	6.72	6.74

In order to be able to calculate this cross section we have modified the formalism of Ref. [4] in such a way that the contribution of nuclear excited states above the threshold energies for proton or neutron emission $E^N_{\rm thres}$ (see Table III [24]) is excluded. This was done by setting the integrand of Eq. (6) to zero when

$$E_\nu - E_e > Q + E^N_{\rm thres} + V_C \tag{15}$$

with $E^N_{\rm thres}$, the smallest of the values $E^p_{\rm thres}$, $E^n_{\rm thres}$, for proton or neutron emission.

In Table II we have computed the ν_e cross sections averaged over the Michel distribution for several nuclei and we show the results of the total cross section and those of the radiochemical cross sections. The ^{12}N nucleus has a very low proton emission threshold which makes it unsuitable for such kind of radiochemical experiment, but all the other nuclei quoted in the Table I can in principle qualify for such an experiment and we have evaluated this cross section.

We can compare our results with those of the recent radiochemical experiment at LAMPF [11] for ^{127}I. The experimental results quoted in [11] give a cross section of

$$\bar{\sigma} = (6.2 \pm 2.5) \times 10^{-40} \ \text{cm}^2.$$

We get a value of

$$\bar{\sigma} = 4.2 \times 10^{-40} \ \text{cm}^2$$

for this cross section. It is also interesting to compare our results with two other recent theoretical results. On the one hand, in Ref. [25] the values

$$\bar{\sigma} = 6.4 \times 10^{-40} \ \text{cm}^2$$

and

$$\bar{\sigma} = 3.0 \times 10^{-40} \ \text{cm}^2$$

are quoted using two different approaches, which rely both on the closure approximation. We should recall, however, that these are total cross sections and not radiochemical. They should be compared to our results in Table II of $\bar{\sigma} = 7.3 \times 10^{-40}$ cm^2.

On the other hand, in Ref. [3] the authors evaluate a genuine radiochemical cross section by summing over the discrete excited states of ^{127}Xe. They obtain a cross section of $\bar{\sigma} = 2.1 \times 10^{-40}$ cm^2, if $g_A = -1.0$ is used, or $\bar{\sigma} = 3.1 \times 10^{-40}$ cm^2, if $g_A = -1.26$ is used. Our method provides an automatic renormalization of g_A by means of the ph and Δh RPA excitation which leads to quenched values of g_A [19]. Hence, the results of Ref. [3], are about a factor of 2 smaller than ours.

There is another recent experimental information which can be contrasted with our predictions. In a recent experiment at Los Alamos with muon neutrinos [13], they obtain the cross section

$$\bar{\sigma} = [8.3 \pm (\text{stat}) \pm 1.6(\text{syst})] \times 10^{-40} \ \text{cm}^2$$

averaged over the ν_μ flux in the range of $123.7 < E_\nu < 280$ MeV for the ^{12}C$(\nu_\mu,\mu^-)X$ reaction. Averaging over the same distribution we obtain a cross section of $\bar{\sigma} = 19 \times 10^{-40}$ cm^2. We should recall that this experiment corrects considerably the previous data of Ref. [12]. Our values here are a bit smaller than the $\bar{\sigma} = 25 \times 10^{-40}$ cm^2 quoted in Ref. [4], because the ν_μ distribution of Ref. [13] has less strength at high energies than the one quoted in [12], which was used to evaluate the results of Ref. [4]. It is also interesting to compare these results with another recent theoretical calculation [26] which uses a continuum random phase approximation calculation and which provides the value $\bar{\sigma} = 20 \times 10^{-40}$ cm^2.

V. SUMMARY AND CONCLUSIONS

In the present work we have done a systematic study of the charged current neutrino- and antineutrino-nucleus inclusive and semi-inclusive cross sections for intermediate energies 20 MeV$\leqslant E_\nu \leqslant$500 MeV. We have chosen a set of eight nuclei which are very important from an experimental point of view in ongoing experiments and current proposals. We have used a reliable method which is based on the local density approximation in finite nuclei and uses the modified Lindhard function to take into account the effects of the Pauli blocking and Fermi motion into the nuclear medium and the finite gap for a minimum nuclear excitation energy. It also takes into consideration the renormalization of the currents involved in the process and the distortion of the outgoing charged lepton due to the Coulomb field.

The method is considerably easier technically than other accurate methods, such as the direct sum over excited states or continuum RPA calculations, and allows a straightforward evaluation in any nucleus. The method is also very accurate (a thorough discussion and comparison with other methods was done in Ref. [4]) and can be used to make further predictions in other isotopes of interest.

We made comparisons of our results with existing data on inclusive cross sections for the ^{12}C$(\nu_e,e^-)X$ reaction measured at LAMPF and KARMEN, and the agreement is good. We also made a comparison with a recent radiochemical experiment for the ^{127}I$(\nu_e,e^-)^{127}$Xe reaction and found our

results to be compatible with experiment within experimental errors.

On the other hand, the cross section for the $^{12}C(\nu_\mu,\mu^-)X$ reaction, which we obtain, is about a factor of 2 bigger than that of a recent experiment at LAMPF and essentially equal to other recent theoretical calculations for the same reaction.

Although, some discrepancies with experiment still remain, as shown in the last example, more serious disagreements found in the past, have been overcome with the advent of new refined experiments. This strengthens our confidence in the method we use to evaluate neutrino cross sections and makes the predictions made here for different nuclei a very valuable information to be used in future experiments or in the calibration of new neutrino detectors.

ACKNOWLEDGMENTS

We would like to thank G. Drexlin and P. Vogel from whom we got useful and timely information and J. D. Vergados for useful discussions. This work has been partially supported by CICYT Contract No. AEN-93-1205. We would like to acknowledge support from the EU Human Capital and mobility Program CHRX-CT 93-0323 and one of us (E.O.) from the Humbolt Foundation.

[1] R. Davis, Jr., D. S. Harmer, and K. C. Hoffman, Phys. Rev. Lett. **20**, 1205 (1968); G. S. Hurst *et al.*, *ibid*. **53**, 1116 (1984); R. Davis, Prog. Part. Nucl. Phys. **32**, 13 (1994).

[2] R. S. Raghavan, Phys. Rev. Lett. **37**, 259 (1976); J. N. Bahcall, *ibid.* **40**, 1351 (1978); W. C. Haxton, *ibid.* **60**, 768 (1988).

[3] J. Engel, S. Pittel, and P. Vogel, Phys. Rev. Lett. **67**, 426 (1991); Phys. Rev. C **50**, 1702 (1994).

[4] S. K. Singh and E. Oset, Phys. Rev. C **48**, 1246 (1993).

[5] J. N. Bahcall and R. K. Ulrich, Rev. Mod. Phys. **60**, 297 (1988); K. Kubodera and S. Nozawa, Int. J. Mod. Phys. E **3**, 101 (1994).

[6] A. I. Abazov *et al.*, Phys. Rev. Lett. **67**, 3332 (1991); P. Anselmann *et al.*, Phys. Lett. B **285**, 376 (1992); K. S. Hirata *et al.*, Phys. Rev. Lett. B **63**, 16 (1989).

[7] J. Rapaport *et al.*, Phys. Rev. Lett. **47**, 1518 (1981); **54**, 2325 (1985); D. Krofcheck *et al.*, *ibid*. **55**, 1051 (1985); Phys. Lett. B **189**, 299 (1987); Yu. S. Lutostansky and N. B. Skul'gina, Phys. Rev. Lett. **67**, 430 (1991).

[8] B. Bodmann *et al.*, Phys. Lett. B **280**, 198 (1992).

[9] B. Zeitnitz, Prog. Part. Nucl. Phys. **32**, 351 (1994).

[10] D.A. Krakauer *et al.*, Phys. Rev. C **45**, 2450 (1992).

[11] B. T. Cleveland, T. Daily, J. Distel, K. Lande, and C. K. Lee *et al.*, in *Proceedings of the 23rd International Cosmic Ray Conference*, University of Calgary, Alberta, Canada, 1993, edited by D. A. Leahy, R. B. Hicks, and D. Venkatesan (World Scientific, Singapore, 1993), Vol. 3, p. 865.

[12] D. D. Koetke *et al.*, Phys. Rev. C **46**, 2554 (1992).

[13] M. Albert *et al.*, Phys. Rev. C **51**, R1065 (1995).

[14] T. W. Donnelly and J. D. Walecka, Phys. Lett. **41B**, 275 (1972); T. W. Donnelly, *ibid.* **43B**, 93 (1973); J. B. Langworthy, B. A. Lamers, and H. Uberall, Nucl. Phys. **A280**, 351 (1977); E. V. Bugaev *et al.*, *ibid*. **A324**, 350 (1979).

[15] B. Goulard and H. Primakoff, Phys. Rev. **135**, B1139 (1964). J. S. Bell and C. H. Llewellyn Smith, Nucl. Phys. **B28**, 317 (1971).

[16] T. K. Gaisser and J. S. O'Connell, Phys. Rev. D **34**, 822 (1986); T. Kuramoto, M. Fukugita, Y. Kohyama, and K. Kubodera, Nucl. Phys. **A512**, 711 (1990).

[17] S. K. Singh and E. Oset, Nucl. Phys. **A542**, 587 (1992); T. S. Kosmas and E. Oset, in *Proceedings of 5th Hellenic Symposium on Nuclear Physics*, Patras, Greece, 1994, edited by K. Syros (World Scientific, Singapore, in press).

[18] H. C. Chiang, E. Oset, and P. Fernandez de Cordoba, Nucl. Phys. **A510**, 591 (1990); H. C. Chiang, E. Oset, R. C. Carrasco, J. Nieves, and J. Navarro, *ibid*. **A510**, 573 (1990).

[19] E. Oset and M. Rho, Phys. Rev. Lett. **42**, 47 (1979).

[20] E. Oset, P. Fernandez de Cordoba, L. L. Salcedo, and R. Brockmann, Phys. Rep. **188**, 79 (1990).

[21] E. Oset, D. Strottman, H. Toki, and J. Navarro, Phys. Rev. C **48**, 2395 (1993).

[22] A. L. Fetter and J. D. Walecka, *Quantum Theory of Many Particle Systems* (McGraw-Hill, New York, 1971).

[23] H. de Vries, C. W. de Jager, and C. de Vries, At. Data Nucl. Data Tables **36**, 495 (1987).

[24] C. M. Lederer and V. S. Shirley, *Tables of Isotopes* (Wiley, New York, 1978).

[25] S. L. Mintz and M. Pourkaviani, Nucl. Phys. **A584**, 665 (1995).

[26] E. Kolbe, K. Langanke, and S. Krewald, Phys. Rev. C **51**, 1122 (1995).